Journal of Medicinal and Chemical Sciences 5 (2022) 887-899

Journal of Medicinal and Chemical Sciences

Journal homepage: http://www.jmchemsci.com/

Original Article

Synthesis and Antidiabetic Assessment of New Coumarin-Disubstituted Benzene Conjugates: An *In Silico–In Virto* Study

Sara Firas Jasim*, Yasser Fakri Mustafa

Department of Pharmaceutical Chemistry, College of Pharmacy, University of Mosul, Ninavah-41002, Iraq

ARTICLE INFO

Article history

Received: 2022-03-29
Received in revised: 2022-04-05
Accepted: 2022-04-14
Manuscript ID: JMCS-2203-1458
Checked for Plagiarism: **Yes**
Language Editor:
Dr. Fatimah Ramezani
Editor who approved publication:
Dr. Ali H. Jawad Al-Taie

DOI:10.26655/JMCHEMSCI.2022.6.3

KEYWORDS

Coumarin-disubstituted benzene conjugates
Antidiabetic
Antioxidative
In-silico

ABSTRACT

Even with the significant advancements in medical and therapeutical fields, finding efficient anti-diabetic and anti-oxidative entities is of high significance in the recent era. New coumarin-disubstituted benzene conjugates were prepared to evaluate their antidiabetic and antioxidative effects. The prepared conjugates (**MT0-MT7**) were characterized utilizing various analytical techniques, including FTIR, UV–Vis, ^{1}H-NMR, and ^{13}C-NMR. Also, the drug-likeness properties of conjugates were assessed *in-silico*. The antidiabetic effect of the prepared conjugates was estimated *in-vitro* based on their inhibitory impact on porcine α-amylase and yeast α-glucosidase enzymes; whereas their antioxidative effect was appraised *in-vitro* based on their snaring impact on hydroxide and DPPH radicals. The findings of evaluating these effects demonstrated that the **MT2** and **MT3** conjugates had a prominent antidiabetic effect related to the standard. In addition, the **MT0** conjugate showed a distinct antioxidative effect comparable to that of the standard. Thus, **MT2**, **MT3**, and **MT0** conjugates could be used as scaffolds to develop a new class of antidiabetic and antioxidative entities. Moreover, the *in-silico* analysis revealed that the majority of the prepared conjugates had convenient drug-likeness properties for the oral drug-delivery system.

GRAPHICAL ABSTRACT

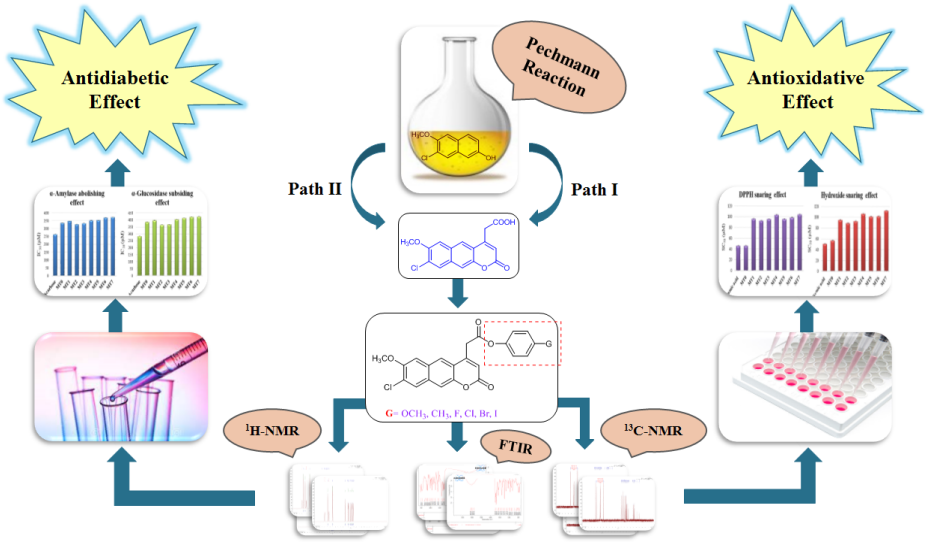

* Corresponding author: Sara Firas Jasim
✉ E-mail: Email: sara.20php6@student.uomosul.edu.iq

Introduction

One of the top-most momentous illnesses in the world is type 2 diabetes, despite the continuous attempts to accommodate it. It is caused primarily by different behavioral, environmental, and genetic agents. By 2040, its incidence is expected to rise to 642 million adults. Hyperglycemia and insulin resistance are hallmarks of type 2 diabetes, which eventually lead to a slew of long-term health problems as the disease progresses. These problems include renal and hepatic failure, neurological, retinal, and cardiovascular diseases [1]. Controlling hyperglycemia via targeting the inhibition of enzymes in the carbohydrate hydrolysis process, like α-glucosidase and α-amylase, is one of the most effective treatment approaches for type 2 diabetes which should be considered [2]. Accordingly, it's paramount to find potent hypoglycemic entities which act as the inhibitors of these enzymes with a good efficacy, selectivity, and safety. The derivation of these entities from different heteroaromatic molecules is a profound issue nowadays [3,4].

In biological systems, the oxidative stress is a complex state in which the formation of free reactive moieties is ungovernable and the capacity of the body to snare and eradicate these reactive moieties via both endogenous and exogenous antioxidative mechanisms is insufficient [5]. According to several studies conducted on humans, a fierce link has been found between oxidative stress and the onset or the development of many illnesses, such as cancer, diabetes mellitus, cardiovascular disease, and others. These findings highlight the importance of striking an optimal balance between free reactive moieties and antioxidants to prevent the consequential physiological and pathological impacts [6]. The antioxidants are considered as a remedy for the harm caused by these free damaging moieties. Nonetheless, due to severe side effects and low efficacy, just a small number of antioxidants have been authorized for clinically usage to date. Consequently, the novel and more efficient antioxidants with minimal side effects are urgently required [7].

The coumarins are members of a large hetero-aromatic family [8]. They are intriguing molecules for many fields of the study due to the conjugated systems found in their fused rings [9]. Coumarin compounds are utilized in industry as additives in food and as ingredients in perfumes and cosmetics, as well. However, its most prominent usage is to synthesize different products in the pharmaceutical industry [10]. Coumarins, from natural and/or synthetic sources, have different biomedical potentials, such as antidiabetic [11], antiviral [12,13], antitubercular [14,15], antifungal [16–19], anticoagulant [20–22], anticancer [23–27], antibacterial [28–32], and antioxidant [33] properties. Moreover, these molecules have many appealing characteristics, such as low toxicity, high bioavailability, simple structure, and low molecular weight, which confirm that they could play a significant role in drug development and research [34–37].

Benzocoumarins, also known as benzochromenones, are a prime bioactive fused-coumarin class. In the past few years, numerous researchers have concentrated their endeavors on isolating, synthesizing, and studying the bioactivities of these coumarin-based compounds due mainly to their expander system of π-conjugation compared to coumarins [38]. These studies revealed that the compounds with a benzocoumarin core have various biomedical properties, including antidiabetic, antimicrobial, anticancer, antioxidant, and antidyslipidemic activities [39]. The antidiabetic and antioxidative properties have taken on importance among the examined activities. As a result, benzocoumarins could serve as the structural templates for promising antidiabetic and antioxidative entities [1,40].

This study aimed to prepare new coumarin-disubstituted benzene conjugates. An *in-silico* study was performed utilizing a pre-ADMET predictor, an online server to analyze the pharmacokinetic parameters and drug-likeness of the prepared conjugates. The antidiabetic effect was estimated *in-vitro* by screening the inhibition impact of the prepared coumarin-disubstituted benzene conjugates on porcine α-amylase (PAA) and yeast α-glucosidase (YAG) enzymes, which regulate the levels of glucose in the blood. Besides, the antioxidative effect of the prepared coumarin-

disubstituted benzene conjugates was screened *in-vitro* by utilizing DPPH and hydroxide radicals, which were used to assess the capacity of the prepared conjugates to snare free reactive moieties.

Materials and Methods

Devices and Chemicals

Chemical compounds, solvents, and reagents used to prepare coumarin-disubstituted benzene conjugates, as well as the biological evaluation systems, were procured from some international resources, such as Haihang, Bioworld, Chem-Lab, Labcorp, Sigma-Aldrich, Scharlau, and others. The procured chemical and biological agents were employed directly without further purification. An ultrasonic-water bath (40 kHz, 350 W, Power Sonic410, Korea) was operated as a sonication system. A digital electrothermal apparatus (CIA9300) was utilized to measure the melting temperatures (Mp) of the prepared coumarin-disubstituted benzene conjugates without pre-correction via an open-capillary approach. The synthesis status progression was checked, and the purity of the prepared conjugates was determined using thin-layer chromatography (TLC). An aluminum-based silica gel sheet (F254) and a mixture of chloroform: methyl alcohol (4:1) served as the fixed and moveable phases in this technique. Likewise, the spectrometers which were involved Bruker-α- ATR-FTIR and UV-1600PC UV-Vis were operated to record the prepared coumarin-disubstituted benzene conjugates' spectra of FTIR and UV, respectively. While the spectra of the prepared conjugates of ^{13}C- and ^{1}H-NMR were obtained utilizing DMSO-*d6* as a solvent on Bruker Avance DRX-75 and -300 MHz, respectively.

Catalog of Chemical Synthesis

The steps of the chemical pathway for preparing coumarin-disubstituted benzene conjugates from 6-amino-7-chloronaphthalen-2-ol are depicted in Scheme 1.

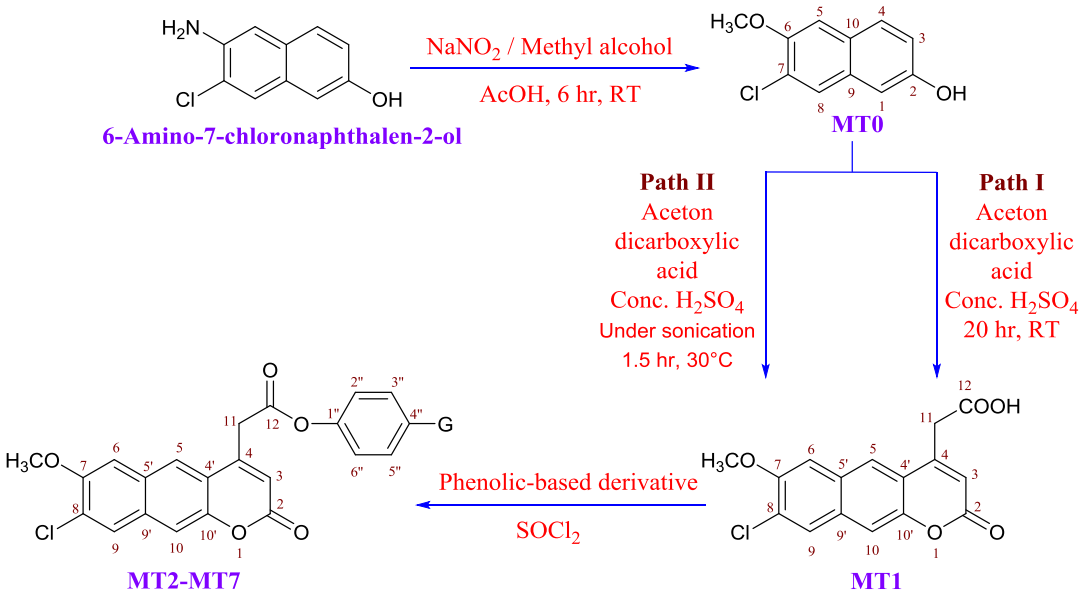

MT2: G= OCH_3; **MT3**: G= CH_3; **MT4**: G= F;
MT5: G= Cl; **MT6**: G= Br; **MT7**: G= I

Scheme 1: The catalog of chemical synthesis of coumarin-disubstituted benzene conjugates.

Synthesis of MT0

At room temperature (RT), 6-amino-7-chloronaphthalen-2-ol (1.930 g, 10.00 mmol), and nitric acid sodium salt (3.450 g, 50.00 mmol) were mixed and stirred for 15 minutes in 90.00 mL of methyl alcohol. At that temperature, 11.50 mL of ethanoic acid was slowly added to the resultant solution, and the stirring was continued strenuously for 6 hours. The gathered solid product was re-crystalized from an aqueous EtOH solution after vaporizing the solvent [41].

7-Chloro-6-methoxynaphthalen-2-ol (**MT0**): French pink; Yield= 43% (0.89 g); Mp= 160-162 °C; R_f = 0.23; λ_{max} (EtOH)= 517 nm; IR: ν_{max}= 916 (s, C-Cl), 1073, 1281 (s, ether C-O-C), 1561 (s, aromatic C=C), 2957 (w, alkyl C-H), 3076 (m,

aromatic C-H), 3300 (br, phenolic O-H) cm^{-1}; ^{1}H-NMR: δ= 4.02 (3H, s, 6-OCH_3), 5.56 (1H, s, 2-OH), 7.22 (1H, d, *J*= 9 Hz, 3-H), 7.33 (1H, s, 5-H), 7.48 (1H, s, 1-H), 7.62 (1H, s, 8-H), 8.08 (1H, d, *J*= 9 Hz, 4-H) ppm; ^{13}C-NMR: δ= 50.1 (CH_3, OCH_3-6), 108.6 (CH, C-5), 111.4 (CH, C-1), 120.2 (CH, C-3), 126.9 (C, C-7), 128.5 (CH, C-8), 129.8 (C, C-10), 131.4 (CH, C-4), 133.1 (C, C-9), 155.7 (C, C-2), and 157.1 (C, C-6) ppm.

Synthesis of Conjugate MT1

Path I

With the assistance of heating, **MT0** (2.750 g, 13.18 mmol) was dissolved in acetone dicarboxylic acid (3.50 mL, 15.00 mmol). After that, the resulting solution was dropped very slowly from a separatory funnel into 25.00 mL of pre-cooled concentrated H_2SO_4 submerged in a bath of ice. During the addition, the reaction mixture was stirred, and the temperature was kept under 10.0 °C. Then, the reaction mixture was retained at RT for 20 hours with continuous stirring before being shed over the ice/water combination. The precipitate was filtered off and rinsed perfectly with cooled water [42].

Path II

Through heating, **MT0** (2.750 g, 13.18 mmol) was dissolved in acetone dicarboxylic acid (3.50 mL, 15.00 mmol). After that, the resulting solution was dropped subsequently from a separatory funnel into 25.00 mL of pre-cooled concentrated H_2SO_4 submerged in a bath of ice. During the addition, the reaction mixture was stirred, and the temperature was kept under 10.0 °C. The reaction mixture was then settled under sonication for 1.5 hours at 30.0 °C before being shed over an ice/water mixture. The precipitate was filtered off and purified by washing with cooled water [43,44].

11-(8-Chloro-7-methoxy-2-oxo-2*H*-benzo[*g*]chromen-4-yl)acetic acid (**MT1**): Yellowish powder; Yield= 79.76% (3.35 g in path I) and 88.09% (3.70 g in path II); Mp= 186-188 °C; R_f = 0.19; λ_{max} (EtOH)= 467 nm; IR: ν_{max}= 941 (s, C-Cl), 1046, 1247 (s, ether C-O-C), 1548 (m, aromatic C=C), 1590 (s, *cis*-alkene C=C), 1692 (s, carboxylic acid C=O), 1734 (s, lactonic ester C=O), 2891 (w, alkyl C-H), 2957 (w, methoxy C-H), 3015 (br, carboxylic acid O-H), 3062 (w, *cis*-alkene C-H) cm^{-1}; ^{1}H-NMR: δ= 3.12 (2H, s, 11-H), 4.03 (3H, s, 7-OCH_3), 6.35 (1H, s, 3-H), 7.12 (1H, s, 10-H), 7.43 (1H, s, 6-H), 7.60 (1H, s, 9-H), 7.92 (1H, s, 5-H), 11.09 (1H, s, 12-OH) ppm; ^{13}C-NMR: δ= 30.9 (CH_2, C-11), 50.1 (CH_3, OCH_3-7), 109.4 (CH, C-6), 113.4 (CH, C-10), 115.8 (CH, C-3), 124.5 (C, C-8), 125.1 (CH, C-5), 126.4 (CH, C-9), 127.5 (C, C-4'), 128.1 (C, C-5'), 130.2 (C, C-9'), 151.8 (C, C-10'), 153.0 (C, C-4), 154.4 (C, C-7), 162.2 (C, C-2), and 173.1 (C, C-12) ppm.

Synthesis of Conjugates MT2-MT7

The conjugate of **MT1** (1.593 g, 5.00 mmol) was added to refreshed $SOCl_2$ (25.00 mL) in a twin-neck flask and submerged in a salted ice bath. A condenser fitted the middle neck, whereas a plug furnished with blue litmus-paper plugged the other. In moisture-less environment, the mixture was stirred gently for half an hour, then at RT for the rest 30 minutes. This was followed by 3 hours of refluxing. The reaction progression was tracked by the litmus-paper color change, which was renewed every 30 minutes. The distillation of $SOCl_2$ excess when the litmus paper blue color remained unchanged gave the alkanoyl chloride intermediate in the flask bottom as a solid white product [45].

At RT, a solution of phenolic-based derivative (4.80 mmol) and azabenzene (1.00 mL) in 50.00 mL of anhydrous ethoxyethane was poured into the same flask housing the white crude. The mixture was agitated for 30 minutes in moisture-less environment. According to the change in litmus-paper color, the reaction was refluxed for a while, as mentioned previously. Then, 50.00 mL of water was added to the mixture when the reaction was completed, followed by separating, dehydrating, and evaporating the organic layer. The conjugates of **MT1** were recrystallized from a CH_2Cl_2: dimethylketone (2:1) mixture [45].

4''-Methoxyphenyl 11-(8-chloro-7-methoxy-2-oxo-2*H*-benzo[*g*]chromen-4-yl)acetate (**MT2**): White powder; Yield= 76.27% (1.62 g); Mp= 171-173 °C; R_f = 0.63; λ_{max} (EtOH)= 331 nm; IR: ν_{max}= 985 (s, C-Cl), 1028, 1266 (s, ether C-O-C), 1595 (s, aromatic C=C), 1665 (s, *cis*-alkene C=C), 1710 (s, ester C=O), 1731 (s, lactonic ester C=O), 2821 (w, alkyl C-H), 2917 (m, methoxy C-H), 3096 (m, *cis*-

alkene C-H) cm^{-1}; ^{1}H-NMR: δ= 3.12 (2H, s, 11-H), 4.03 (3H, s, 7-OCH_3), 4.12 (3H, s, 4''-OCH_3), 6.35 (1H, s, 3-H), 6.74 (2H, d, *J*= 6 Hz, 2''-, 6''-H), 7.01 (2H, d, *J*= 6 Hz, 3''-, 5''-H), 7.12 (1H, s, 10-H), 7.43 (1H, s, 6-H), 7.60 (1H, s, 9-H), 7.92 (1H, s, 5-H) ppm; ^{13}C-NMR: δ= 28.3 (CH_2, C-11), 50.1 (CH_3, OCH_3-7), 51.1 (CH_3, OCH_3-4''), 109.4 (CH, C-6), 112.3 (CH, C-2'', -6''), 113.4 (CH, C-10), 115.8 (CH, C-3), 120.1 (CH, C-3'', -5''), 124.5 (C, C-8), 125.1 (CH, C-5), 126.4 (CH, C-9), 127.5 (C, C-4'), 128.1 (C, C-5'), 130.2 (C, C-9'), 144.6 (C, C-1''), 151.8 (C, C-10'), 153.0 (C, C-4), 154.4 (C, C-7), 156.4 (C, C-4''), 162.2 (C, C-2), and 169.5 (C, C-12) ppm.

4''-Tolyl 11-(8-chloro-7-methoxy-2-oxo-2*H*-benzo[*g*]chromen-4-yl)acetate (**MT3**): Off-white powder; Yield= 74.36% (1.52 g); Mp= 156-158 °C; R_f = 0.58; λ_{max} (EtOH)= 378 nm; IR: ν_{max}= 985 (s, C-Cl), 1030, 1267 (s, ether C-O-C), 1597 (s, aromatic C=C), 1668 (s, *cis*-alkene C=C), 1713 (s, ester C=O), 1733 (s, lactonic ester C=O), 2819 (w, alkyl C-H), 2912 (w, methoxy C-H), 3090 (m, *cis*-alkene C-H) cm^{-1}; ^{1}H-NMR: δ= 2.75 (3H, s, 4''-CH_3), 3.12 (2H, s, 11-H), 4.02 (3H, s, 7-OCH_3), 6.35 (1H, s, 3-H), 7.02 (2H, d, *J*= 6 Hz, 2''-, 6''-H), 7.12 (1H, s, 10-H), 7.25 (2H, d, *J*= 6 Hz, 3''-, 5''-H), 7.43 (1H, s, 6-H), 7.60 (1H, s, 9-H), 7.92 (1H, s, 5-H) ppm; ^{13}C-NMR: δ= 24.1 (CH_3, CH_3-4''), 27.5 (CH_2, C-11), 50.1 (CH_3, OCH_3-7), 109.4 (CH, C-6), 113.4 (CH, C-10), 115.8 (CH, C-3), 119.0 (CH, C-2'', -6''), 122.0 (CH, C-3'', -5''), 124.5 (C, C-8), 125.1 (CH, C-5), 126.4 (CH, C-9), 127.5 (C, C-4'), 128.1 (C, C-5'), 130.2 (C, C-9'), 134.2 (C, C-4''), 149.3 (C, C-1''), 151.8 (C, C-10'), 153.0 (C, C-4), 154.4 (C, C-7), 162.2 (C, C-2), and 169.5 (C, C-12) ppm.

4''-Fluorophenyl 11-(8-chloro-7-methoxy-2-oxo-2*H*-benzo[*g*]chromen-4-yl)acetate (**MT4**): White powder; Yield= 69.28% (1.43 g); Mp= 166-168 °C; R_f = 0.42; λ_{max} (EtOH)= 330 nm; IR: ν_{max}= 986 (s, C-Cl), 1077 (s, C-F), 1028, 1266 (s, ether C-O-C), 1597 (s, aromatic C=C), 1666 (s, *cis*-alkene C=C), 1711 (s, ester C=O), 1733 (s, lactonic ester C=O), 2820 (w, alkyl C-H), 2918 (w, methoxy C-H), 3070 (m, *cis*-alkene C-H) cm^{-1}; ^{1}H-NMR: δ= 3.12 (2H, s, 11-H), 4.02 (3H, s, 7-OCH_3), 6.35 (1H, s, 3-H), 7.04 (2H, d, *J*= 6 Hz, 3''-, 5''-H), 7.12 (1H, s, 10-H), 7.26 (2H, d, *J*= 6 Hz, 2''-, 6''-H), 7.43 (1H, s, 6-H), 7.60 (1H, s, 9-H), 7.92 (1H, s, 5-H) ppm; ^{13}C-NMR: δ= 27.5 (CH_2, C-11), 50.1 (CH_3, OCH_3-7), 108.5 (CH, C-3'', -5''), 109.4 (CH, C-6), 113.4 (CH, C-10), 115.8 (CH, C-3), 120.7 (CH, C-2'', -6''), 124.5 (C, C-8), 125.1 (CH, C-5), 126.4 (CH, C-9), 127.5 (C, C-4'), 128.1 (C, C-5'), 130.2 (C, C-9'), 147.9 (C, C-1''), 151.8 (C, C-10'), 153.0 (C, C-4), 154.4 (C, C-7), 158.7 (C, C-4''), 162.2 (C, C-2), and 169.5 (C, C-12) ppm.

4''-Chlorophenyl 11-(8-chloro-7-methoxy-2-oxo-2*H*-benzo[*g*]chromen-4-yl)acetate (**MT5**): White powder; Yield= 68.50% (1.47 g); Mp= 158-160 °C; R_f = 0.46; λ_{max} (EtOH)= 341 nm; IR: ν_{max}= 985 (s, C-Cl), 1031, 1265 (s, ether C-O-C), 1595 (s, aromatic C=C), 1667 (s, *cis*-alkene C=C), 1710 (s, ester C=O), 1730 (s, lactonic ester C=O), 2820 (w, alkyl C-H), 2916 (w, methoxy C-H), 3068 (m, *cis*-alkene C-H) cm^{-1}; ^{1}H-NMR: δ= 3.12 (2H, s, 11-H), 4.02 (3H, s, 7-OCH_3), 6.35 (1H, s, 3-H), 7.12 (1H, s, 10-H), 7.35 (2H, d, *J*= 6 Hz, 2''-, 6''-H), 7.43 (1H, s, 6-H), 7.53 (2H, d, *J*= 6 Hz, 3''-, 5''-H), 7.60 (1H, s, 9-H), 7.92 (1H, s, 5-H) ppm; ^{13}C-NMR: δ= 33.2 (CH_2, C-11), 50.1 (CH_3, OCH_3-7), 109.4 (CH, C-6), 113.4 (CH, C-10), 115.8 (CH, C-3), 120.5 (CH, C-2'', -6''), 122.9 (CH, C-3'', -5''), 124.5 (C, C-8), 125.1 (CH, C-5), 126.4 (CH, C-9), 127.5 (C, C-4'), 128.1 (C, C-5'), 130.2 (C, C-9'), 132.0 (C, C-4''), 150.4 (C, C-1''), 151.8 (C, C-10'), 153.0 (C, C-4), 154.4 (C, C-7), 162.2 (C, C-2), and 169.5 (C, C-12) ppm.

4''-Bromophenyl 11-(8-chloro-7-methoxy-2-oxo-2*H*-benzo[*g*]chromen-4-yl)acetate (**MT6**): White powder; Yield= 62.50% (1.48 g); Mp= 142-144 °C; R_f = 0.49; λ_{max} (EtOH)= 335 nm; IR: ν_{max}= 900 (s, C-Br), 986 (s, C-Cl), 1023, 1262 (s, ether C-O-C), 1593 (s, aromatic C=C), 1664 (s, *cis*-alkene C=C), 1709 (s, ester C=O), 1732 (s, lactonic ester C=O), 2819 (w, alkyl C-H), 2913 (w, methoxy C-H), 3066 (m, *cis*-alkene C-H) cm^{-1}; ^{1}H-NMR: δ= 3.13 (2H, s, 11-H), 4.02 (3H, s, 7-OCH_3), 6.35 (1H, s, 3-H), 6.95 (2H, d, *J*= 6 Hz, 2''-, 6''-H), 7.11 (1H, s, 10-H), 7.43 (1H, s, 6-H), 7.60 (1H, s, 9-H), 7.77 (2H, d, *J*= 6 Hz, 3''-, 5''-H), 7.92 (1H, s, 5-H) ppm; ^{13}C-NMR: δ= 33.2 (CH_2, C-11), 50.1 (CH_3, OCH_3-7), 109.4 (CH, C-6), 113.4 (CH, C-10), 115.8 (CH, C-3), 118.5 (C, C-4''), 121.3 (CH, C-2'', -6''), 123.6 (CH, C-3'', -5''), 124.5 (C, C-8), 125.1 (CH, C-5), 126.4 (CH, C-9), 127.5 (C, C-4'), 128.1 (C, C-5'), 130.2 (C, C-9'), 151.3 (C, C-1''), 151.8 (C, C-10'), 153.0 (C, C-4), 154.4 (C, C-7), 162.2 (C, C-2), and 169.5 (C, C-12) ppm.

4''-Iodophenyl 11-(8-chloro-7-methoxy-2-oxo-2*H*-benzo[*g*]chromen-4-yl)acetate (**MT7**): White powder; Yield= 64.54% (1.68 g); Mp= 136-138 °C; R_f = 0.51; λ_{max} (EtOH)= 339 nm; IR: ν_{max}= 866 (s, C-I), 986 (s, C-Cl), 1028, 1265 (s, ether C-O-C), 1592 (s, aromatic C=C), 1661 (s, *cis*-alkene C=C), 1711 (s, ester C=O), 1733 (s, lactonic ester C=O), 2823 (w, alkyl C-H), 2913 (w, methoxy C-H), 3064 (m, *cis*-alkene C-H) cm^{-1}; ^{1}H-NMR: δ= 3.13 (2H, s, 11-H), 4.00 (3H, s, 7-OCH_3), 6.35 (1H, s, 3-H), 6.83 (2H, d, *J*= 6 Hz, 2''-, 6''-H), 7.11 (1H, s, 10-H), 7.43 (1H, s, 6-H), 7.60 (1H, s, 9-H), 7.85 (2H, d, *J*= 6 Hz, 3''-, 5''-H), 7.92 (1H, s, 5-H) ppm; ^{13}C-NMR: δ= 33.2 (CH_2, C-11), 50.2 (CH_3, OCH_3-7), 93.0 (C, C-4''), 109.4 (CH, C-6), 113.4 (CH, C-10), 115.8 (CH, C-3), 120.7 (CH, C-2'', -6''), 124.5 (C, C-8), 125.1 (CH, C-5), 126.4 (CH, C-9), 127.5 (C, C-4'), 128.1 (C, C-5'), 129.6 (CH, C-3'', -5''), 130.2 (C, C-9'), 151.2 (C, C-1''), 151.8 (C, C-10'), 153.0 (C, C-4), 154.4 (C, C-7), 162.2 (C, C-2), and 169.5 (C, C-12) ppm.

Assessment of the Bioactivities

Antidiabetic Effect

Exploiting acarbose (ACA) as a standard, the prepared coumarin-disubstituted benzene conjugates' capacities to subside YAG and abolish PAA were estimated. From a master solution (2.00 mg/mL), seven sub-master solutions of 1000.00, 800.00, 400.00, 200.00, 100.00, 50.00, and 25.00 µg/mL were obtained using DMSO as a thinner. Each inspected conjugate's antidiabetic effect was represented as an inhibitory percent (I%) equivalent to (Abs_{aca} – Abs_{test}/Abs_{aca}) ×100. The absorbance readings for the ACA and the inspected conjugate were symbolized by Abs_{aca} and Abs_{test}, respectively. In nonlinear regression, the I% values were plotted against the logarithmic concentrations to calculate the IC_{50} score. The latter expresses the concentration at which half of the enzymatic activity is inhibited by ACA or the prepared conjugates. The following equation [1 – (IC_{50} of inspected conjugate – IC_{50} of ACA/ IC_{50} of ACA)] was used to compute the potency ratio (PR) of the inspected conjugates [46].

PAA Abolishing Test

In a pH 6.8 phosphate-buffered solution (PBS), the starch was dissolved as a test substrate to obtain the substrate-mixture (2.00 mL of 500.00 µg/mL), while the enzyme-mixture was obtained by mixing an equal volume (20.00 µL) of PAA (2.00 unit/mL) in PBS with a solution of definite concentration of the inspected conjugate. After that, 40.00 µL of the substrate-mixture was mixed with 40.00 µL of the enzyme-mixture, followed by incubation for 10 minutes at 25.0 °C. To the latter, 2.00 mL of the aqueous caustic soda solution (0.40 M) containing dehydrated Rochelle salt (12.00%) and 2-hydroxy-3,5-dinitrobenzoic acid (1.00%) was added to stop the interaction. Then, the resultant solution was readjusted with distilled water to 10.00 mL and refrigerated to 25.0 °C in a bath of crushed ice after 15 minutes of heating in a boiling water bath. At 540.0 nm, the capacity of the resultant solution to abolish the PAA was estimated colorimetrically. The blank solution included all of the preceding additions except the inspected solution, which was substituted by the DMSO [46].

YAG Subsiding Test

In a PBS (pH 6.8), pNP-α-D-glucopyranoside was dissolved as a test substrate to obtain the substrate-mixture (375.00 µg/mL), while the enzyme-mixture was obtained by mixing an equal volume (20.00 µL) of YAG (0.10 unit/mL) in a PBS with a solution of definite concentration of the inspected conjugate. After that, 40.00 µL of the substrate-mixture was mixed with 40.00 µL of the enzyme-mixture, followed by incubation for 30 minutes at 37.0 °C. To the latter, 0.20 M of disodium carbonate in 80.00 µL of PBS was added to stop the interaction. At 405.0 nm, the resultant solution's capacity to subside the YAG was estimated colorimetrically. The blank solution included all of the preceding additions except the inspected solution, which was substituted by the DMSO [46].

Antioxidative Effect

Exploiting cevitamic acid (Vit.C) as a standard, the prepared coumarin-disubstituted benzene conjugates' capacities to transmit an electron in the oxidoreduction reaction and snare the hydroxide and DPPH (2,2-diphenyl-1-picryl-hydrazyl) radicals were estimated. From a master solution (1.00 mg/mL), seven sub-master solutions in a double diluted serial manner, with orders between 400.00 and 6.25 µg/mL, were

acquired using EtOH as a thinner. The antioxidative effect of each inspected conjugate was represented as a snaring percent (S%) equivalent to (Abs_{cev} – Abs_{test}/Abs_{cev}) ×100. The absorbance readings for Vit.C and the inspected conjugate were symbolized by Abs_{cev} and Abs_{test}, respectively. In nonlinear regression, the S% values were plotted against the logarithmic concentrations to calculate the SC_{50} score. The latter expresses the concentration at which half of the ferric ions or reactive moieties are reduced or snared, respectively, by Vit.C or the prepared conjugates [47].

DPPH-Radical Snaring Test

0.50 mL of 0.10 mM alcoholic DPPH solution was initially pipetted into 1.50 mL of the inspected solution at a definite concentration to make the testing combination. After that, the combination was harbored for 0.5 hours at 25.0 °C while being kept out of light by an aluminum shield. At 517.0 nm, the capacity of the resultant solution to exterminate the violet color of DPPH was estimated colorimetrically. An alcoholic DPPH solution (0.50 mL) was added to EtOH (1.50 mL) to obtain the blank solution [48].

Hydroxide-Radical Snaring Test

2.40 mL of a buffer solution of potassium phosphate (pH 7.8, 0.20 M) was primarily pipetted to 1.50 mL of the inspected solution at a definite concentration. Following that, a trichloroiron (60.00 µL, 0.0010 M), 1,10-phenanthroline (90.00 µL of 0.0010 M), and superoxol (150.00 µL of 0.170 M) were pipetted to the previous combination. At 560.0 nm, the snaring capacity of the resultant solution was estimated colorimetrically after harboring for 5 minutes at 25.0 °C. The blank solution of this test included all of the preceding additions, with the exception of the inspected solution, which was substituted by the buffer solution [49].

Drug-Likeness Properties Assessment

The ADME (absorption, distribution, metabolism, and excretion) and drug-likeness of the prepared coumarin-disubstituted benzene conjugates were analyzed utilizing the preADMET predictor server, which depends on the two-dimensional chemical structure of the inspected conjugates [50].

Results and Discussion

Catalog of Chemical Synthesis

As illustrated in Scheme 1, the design and synthesis of coumarin-disubstituted benzene conjugates involved several steps. These steps were initiated with the aromatic nucleophilic substitution reaction by forming a diazonium salt intermediate at the C-6 position of 6-amino-7-chloronaphthalen-2-ol utilizing nitric acid sodium salt, methyl alcohol, and ethanoic acid to produce **MT0**. It is noteworthy that this reaction is novel and was primarily used here to substitute the amino group in the aromatic ring with the methoxy group [41]. Then, by applying two paths based on the Pechmann reaction, a coumarin-disubstituted benzene conjugate, **MT1**, was prepared. The classic Pechmann reaction was chosen for the synthesis of this conjugate because of the starting material's generality and availability, as well as the product's high yield [38].

In path I, the 2-naphthol compound **MT0** was condensed with acetone dicarboxylic acid, affording the coumarin-disubstituted benzene conjugate **MT1** in a good yield of 79.76% by using the concentrated H_2SO_4 as a catalyst at RT for 24 hours [42]. While in path II, the condensation of **MT0** with acetone dicarboxylic acid was achieved using the concentrated H_2SO_4 as a catalyst to produce **MT1** with an excellent yield of 88.09% by employing an ultrasound bath for 1.5 hours at 30.0 °C. It's important to mention that ultrasound-promoted reaction is a green method for chemical synthesis. Moreover, the sonication in path II reduced reaction time and increased the yield percentage [43,44,51].

Finally, the **MT1** carboxylic acid group was transformed by the $SOCl_2$ catalyst to prepare the acyl chloride-based intermediate. Then, different *para*-substituted phenolic compounds reacted with the generated intermediate to obtain the target conjugates (**MT2**-**MT7**) [45]. At the para position of the employed phenols, the group's nature impacted the yield percentage of the prepared conjugates. The good electron-donating group gave the most elevated percentage, whereas the good electron-withdrawing group gave the most decreased percentage. Spectroscopical data

was used to affirm the structures of the prepared conjugates.

Drug-Likeness Properties Assessment

The analysis of the ADME profile of drug candidates is a significant constraint during drug discovery and leads to the compound selection. About 50% of the candidates failed in the development stages due to unacceptable ADME profiles. To avoid this failure, *in-silico* technologies were successfully applied to predict ADME-related properties and provide guidance in the initial stages of drug discovery processes. Besides, studying these properties may aid in choosing the proper lead compounds before conducting *in-vitro* and *in-vivo* studies, which results in saving time and funds [52–54].

The assessment of the obtained results, as listed in Table 1, revealed a number of intriguing points. Initially, the prepared coumarin-disubstituted benzene conjugates had an excellent human intestinal absorption (HIA) in the range of 97.46–98.93% and moderate Caco-2 cell line permeability. These findings indicate that the absorption through the intestine might depend on the other mechanisms besides passive diffusion. This is due to Caco-2 cell models' expression lacking certain transporters, mucus-secretory cells, and non-cellular parameters like bile acids and phospholipids which can also affect the absorption process. Further, tight junctions of the Caco-2 system make it less permeable to the compounds which can be absorbed paracellularly [55–57].

Moreover, **MT2**-**MT7** conjugates inhibited the P-glycoprotein (P-gp) transporter. Hence, they can increase apical-to-basolateral intestinal permeability and bioavailability of drugs that are substrates for this efflux system. Also, the inhibition of the P-gp transporter can lead to several drug-drug interactions in the distribution and elimination processes [58]. In addition, the prepared coumarin-disubstituted benzene conjugates except **MT1** inhibited the CYP3A4 enzyme, which is responsible for metabolizing and eliminating about 50% of marketed drugs, so inhibiting this enzyme will result in a drug-drug interaction [59]. Further, the prepared conjugates inhibited the CYP2C9 enzyme, which may lead to drug-drug interactions with drugs which use this enzyme for their metabolism [60].

Thus, all prepared conjugates except **MT0** had a high plasma protein binding capacity ranging between 89.46–100.00%, resulting in a low volume of distribution, a long plasma half-life, and a low clearance rate. High plasma protein binding capacity can also affect efficacy because only the free fraction of the drug is responsible for pharmacological activity [61]. Likewise, the prepared conjugates were non-permeable across the blood-brain barrier except **MT0**, which was permeable. Brain penetration is a critical factor considered when trying to avoid or target the brain during the designing step. Impermeability of compounds in the blood-brain barrier reduces or eliminates the risk of undesirable CNS side effects and toxicity [62–64].

Finally, role-of-five comprises four physicochemical parameter requirements that determine the drug-likeness for the oral delivery system, which involve the H-bond acceptors ≤ 10, H-bond donors ≤ 5, a molecular mass ≤ 500.0, and log P ≤ 5.0. Generally, orally administered drugs should have no more than one break-up of these requirements to display the good aqueous solubility and intestinal permeability profiles, or else. The absorption and bioavailability are likely to be poor. According to the *in-silico* study, all prepared conjugates except **MT0** complied with Lipinski's rule. As a result, these conjugates have lower attrition rates during drug development and clinical trials and therefore have a better chance of reaching the market [65,66].

Table 1: In-silico-based pharmacokinetic profile of the prepared coumarin-disubstituted benzene conjugates

Conjugate symbol	Role-of-five	BBB-P C.brain/C.blood	PPB %	CYP2C9 blockage	CYP2D6 blockage	CYP3A4 blockage	HIA %	Pgp blockage	Caco2-P nm/sec
MT0	Fit	2.19	19.94	Blocker	Nil	Blocker	97.71	Nil	32.85
MT1	Fit	0.010	89.46	Blocker	Nil	Nil	98.93	Nil	20.16
MT2	Fit	0.07	91.89	Blocker	Nil	Blocker	97.49	Blocker	34.99
MT3	Fit	0.16	92.88	Blocker	Nil	Blocker	97.50	Blocker	34.66
MT4	Fit	0.06	92.91	Blocker	Nil	Blocker	97.46	Blocker	34.80
MT5	Fit	0.08	93.94	Blocker	Nil	Blocker	97.69	Blocker	36.60
MT6	Fit	0.08	96.65	Blocker	Nil	Blocker	97.86	Blocker	34.61
MT7	Not-fit	0.09	100.00	Blocker	Nil	Blocker	98.42	Blocker	33.88

***Role-of-five**: **Lipinski's rule**, **BBB-P**: Blood-brain barrier penetration, **PPB**: Plasma protein binding, **CYP2C9**: Cytochrome-P450 2C9, **CYP2D6**: Cytochrome-P450 2D6, **CYP3A4**: Cytochrome-P450 3A4, **HIA**: Human intestinal absorption, **Pgp**: P-glycoprotein, **Caco2-P**: Caco2 cell permeability (human colorectal carcinoma).*

Valuation of the Bioactivities

Antidiabetic Effect

The capacity of the pure prepared coumarin-disubstituted benzene conjugates to abolish PAA and subside YAG was investigated *in-vitro* to assess their antidiabetic effect using ACA as a standard. The PAA abolishing effect scores of standard and inspected conjugates represented by IC_{50} (μM) ± SD (*n*=3) were as follows: **ACA**= 263.26±0.92, **MT0**= 336.06±0.89, **MT1**= 348.22±0.91, **MT2**= 326.47±0.96, **MT3**= 334.13±0.90, **MT4**= 352.67±0.93, **MT5**= 353.12±1.01, **MT6**= 370.28±0.86, and **MT7**= 372.39±0.98. Whereas the YAG subsiding effect scores of standard and inspected conjugates were as follows: **ACA**= 283.04±0.88, **MT0**= 385.46±0.93, **MT1**= 396.72±1.01, **MT2**= 364.31±0.95, **MT3**= 366.84±0.92, **MT4**= 403.05±0.94, **MT5**= 413.38±0.94, **MT6**= 421.94±0.99, and **MT7**= 424.02±1.02. On the other hand, the PR scores of standard and inspected conjugates towards PAA were as follows: **ACA**= 1.00, **MT0**= 0.72, **MT1**= 0.68, **MT2**= 0.76, **MT3**= 0.73, **MT4**= 0.66, **MT5**= 0.66, **MT6**= 0.59, and **MT7**= 0.59. Whereas the PR scores of standard and inspected conjugates towards YAG were as follows: **ACA**= 1.00, **MT0**= 0.64, **MT1**= 0.60, **MT2**= 0.71, **MT3**= 0.70, **MT4**= 0.58, **MT5**= 0.54, **MT6**= 0.51, and **MT7**= 0.50. The above-mentioned scores are depicted as a diagram in Figure 1.

According to the findings of the study, the prepared conjugates had a moderate antidiabetic effect compared to ACA. The conjugates showed an abolishing impact on PAA and a subsiding impact on YAG, with IC_{50} values ranging between 326.47–372.39 μM and 364.31–424.02 μM, respectively. Likewise, by the observation of the inhibitory map, the authors concluded that the prepared conjugates revealed the same pattern of antidiabetic effect on the two inspected enzymes. The ranking of declining antidiabetic effects matches the order: **MT2**, **MT3**, **MT0**, **MT1**, **MT4**, **MT5**, **MT6**, and **MT7**.

In comparison to the other prepared conjugates, **MT2** and **MT3** exhibited a prominent antidiabetic effect towards PAA and YAG, with a potency related to ACA. The authors assumed this superior impact was due to the existence of electron-donating moieties involved CH_3O and CH_3 at position 4'' in the chemical structures of **MT2** and **MT3**, respectively. The attachment of these moieties to a highly conjugated system can enhance the antidiabetic effect [67]. Thus, **MT2** and **MT3** could be promising scaffolds for the development of efficient antidiabetic entities. Furthermore, the lower antidiabetic impact of

MT4, **MT5**, **MT6**, and **MT7** compared to the other prepared conjugates may be due to the existence of electron-withdrawing moieties involved F, Cl, Br, and I at position 4'' in the chemical structures of **MT4**, **MT5**, **MT6**, and **MT7**, respectively. The incorporation of these moieties into a highly conjugated system can reduce the antidiabetic effect [46,67].

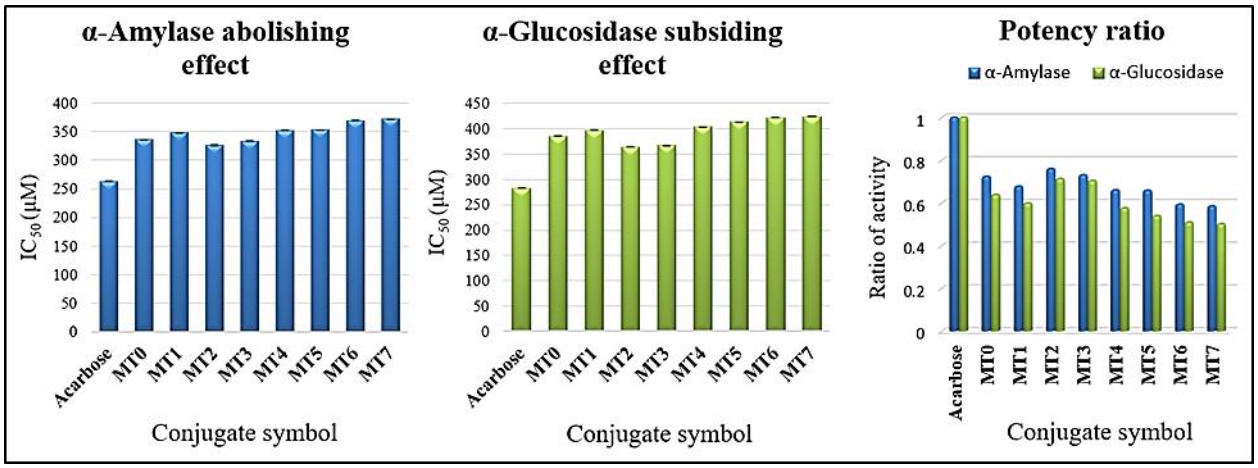

Figure 1: The diagram expresses the parameters of the antidiabetic effect valuation of the prepared coumarin-disubstituted benzene conjugates

Antioxidative Effect

The capacity of the pure prepared coumarin-disubstituted benzene conjugates to snare the DPPH and hydroxide radical moieties *in-vitro* was monitored to evaluate their antioxidative effect. The DPPH-radical snaring effect scores of standard and inspected conjugates represented by SC_{50} (µM) ± SD (*n*=3) were as follows: **Vit.C**= 45.87±1.12, **MT0**= 46.12±1.20, **MT1**= 95.68±1.15, **MT2**= 92.67±1.15, **MT3**= 95.12±0.99, **MT4**= 103.31±1.05, **MT5**= 95.38±1.10, **MT6**= 98.49±1.08, and **MT7**= 104.16±1.14. Whereas the hydroxide-radical snaring effect scores of standard and inspected conjugates were as follows: **Vit.C**= 50.73±0.98, **MT0**= 56.76±1.05, **MT1**= 94.89±1.08, **MT2**= 89.14±1.20, **MT3**= 92.37±1.00, **MT4**= 106.10±1.15, **MT5**= 101.06±1.05, **MT6**= 101.52±1.15, and **MT7**= 112.01±0.96. The above-mentioned scores are illustrated as a diagram in Figure 2.

Based on findings of the study, the prepared conjugates displayed a snaring effect on DPPH and hydroxide radicals but less than Vit.C, with SC_{50} values ranging between 46.12–104.16 µM and 56.76–112.01 µM, respectively. Also, the prepared conjugates exhibited a parallel pattern of snaring the two inspected radicals, which conformed to the following descending order: **MT0**, **MT2**, **MT3**, **MT1**, **MT5**, **MT6**, **MT4**, and **MT7**. This order indicates that as the conjugation system of the prepared conjugates was enhanced with the electron-donating substituents, the antioxidative effect increased.

Conjugate **MT0** demonstrated a greater snaring impact on inspected radicals than other prepared conjugates, with potency comparable to that of Vit.C. The authors attributed this superior effect of **MT0** to the existence of the aromatic OH moiety at position 2 of its chemical structure, which enhances the system's conjugation competence [7]. On the other hand, the lower antioxidative effect of **MT7**, **MT4**, **MT6**, and **MT5** compared to the other prepared conjugates may be due to the existence of halogen moieties at position 4'' of their chemical structures. From the author's perspective, these halogens weaken the conjugation competence of the system as they are electron-withdrawing moieties [68].

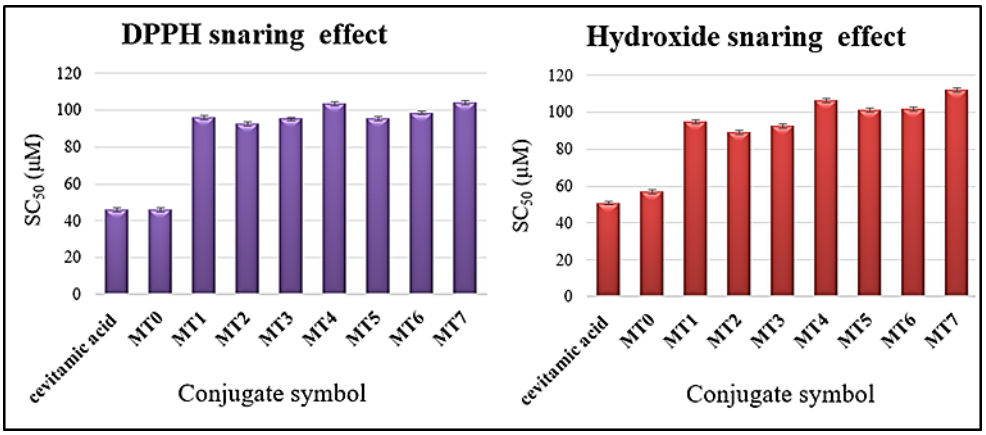

Figure 2: The diagram expresses the parameters of the antioxidative effect valuation of the prepared coumarin-disubstituted benzene conjugates

Conclusion

In the proposed study, new coumarin-disubstituted benzene conjugates were synthesized and valuated *in-vitro* as possible antidiabetic and antioxidative entities. Although the prepared conjugates had a less antidiabetic effect than the standard, two of our conjugates, **MT2** and **MT3**, exhibited a promising inhibitory impact on porcine α-amylase and yeast α-glucosidase. Thus, they could serve as auspicious candidates for the development of a new class of antidiabetic entities. Interestingly, the **MT0** conjugate displayed a distinct snaring impact on the inspected reactive moieties, with potency comparable to that of the standard. Therefore, it could serve as a template to develop a new class of antioxidative entities. Additionally, most of the prepared conjugates had convenient drug-likeness properties for the oral delivery system based on the *in-silico* analysis. As a result, our conjugates may put a spotlight on the design of newer coumarins for the management of diabetes and oxidative stress.

Acknowledgments

The authors gratefully thank the University of Mosul/College of Pharmacy for providing facilities that improved the quality of this work. They are also grateful to Dr. Sarah Ahmed Waheed, Dr. Rahma Mowaffaq Jebir, and Dr. Reem Nadher Ismael for their efforts to improve this work's quality.

Funding

This research did not receive any specific grant from funding agencies in the public, commercial, or not-for-profit sectors.

Authors' contributions

Based on the recommendations of the international Committee of Medical Journal Editors, all authors met the criteria of authorship.

Conflict of Interest

We have no conflicts of interest to disclose.

ORCID:

Sara Firas Jasim
https://orcid.org/0000-0002-7863-3313
Yasser Fakri Mustafa
https://www.orcid.org/0000-0002-0926-7428

References

[1]. Abdul-Ridha N.A., Salmaan A.D., Sabah R., Saeed B., Al-Masoudi N.A., *Z. Naturforsch. B,* 2021, **76**:201 [Crossref], [Google Scholar], [Publisher]

[2]. Tolmie M., Bester M.J., Apostolides Z., *J. Diabetes,* 2021, **13**:779 [Crossref], [Google Scholar], [Publisher]

[3]. Bratenko M., Perepelytsya O., Yaremii I., Kupchanko K., Panasenko N., Vovk M., *Biointerface Res. Appl. Chem.,* 2021, **11**:14403 [Crossref], [Google Scholar], [Publisher]

[4]. Oglah M.K., Mustafa Y.F., *Med. Chem. Res.,* 2020, **29**:479 [Crossref], [Google Scholar], [Publisher]

[5]. Sies H., *Antioxidants,* 2020, **9**:852 [Crossref], [Google Scholar], [Publisher]

[6]. Hayes J.D., Dinkova-Kostova A.T., Tew K.D., *Cancer Cell,* 2020, **38**:167 [Crossref], [Google Scholar], [Publisher]

[7]. Khalil R.R., Mustafa Y.F., *Syst. Rev. Pharm.,* 2020, **11**:57 [Google Scholar], [Publisher]

[8]. Mustafa Y.F., Najem M.A., Tawffiq Z.S., *J. Appl. Pharm. Sci.,* 2018, **8**:49 [Crossref], [Google Scholar], [Publisher]
[9]. Annunziata F., Pinna C., Dallavalle S., Tamborini L., Pinto A., *Int. J. Mol. Sci.,* 2020, **21**:4618 [Crossref], [Google Scholar], [Publisher]
[10]. Carneiro A., Matos M.J., Uriarte E., Santana L., *Molecules,* 2021, **26**:501 [Crossref], [Google Scholar], [Publisher]
[11]. Oglah M.K., Mustafa Y.F., Bashir M.K., Jasim M.H., *Syst. Rev. Pharm.,* 2020, **11**:472 [Google Scholar], [Publisher]
[12]. Mustafa Y.F., Abdulaziz N.T., *Syst. Rev. Pharm.,* 2020, **11**:438 [Google Scholar], [Publisher]
[13]. Jebir R.M., Mustafa Y.F., *Iraqi J. Pharm.,* 2021, **18**:139 [Crossref], [Google Scholar], [Publisher]
[14]. Mustafa Y.F., Khalil R.R., Mohammed E.T., Bashir M.K., Oglah M.K., *Arch. Razi Inst.,* 2021, **76**:1297 [Crossref], [Google Scholar], [Publisher]
[15]. Mustafa Y.F., *J. Glob. Pharma Technol.,* 2019, **11**:1 [Google Scholar], [Publisher]
[16]. Jebir R.M., Mustafa Y.F., *J. Med. Chem. Sci.,* 2022, **5**:652 [Crossref], [Google Scholar], [Publisher]
[17]. Mahmood A.A.J., Mustafa Y.F., Abdulstaar M., *Int. Med. J. Malaysia,* 2014, **13**:3 [Crossref], [Google Scholar], [Publisher]
[18]. Mustafa Y.F., Khalil R.R., Mohammed E.T., *Syst. Rev. Pharm.,* 2020, **11**:382 [Google Scholar], [Publisher]
[19]. Mohammed E.T., Mustafa Y.F., *Syst. Rev. Pharm.,* 2020, **11**:64 [Google Scholar], [Publisher]
[20]. Oglah M.K., Bashir M.K., Mustafa Y.F., Mohammed E.T., Riyadh R., *Syst. Rev. Pharm.,* 2020, **11**:717 [Google Scholar], [Publisher]
[21]. Mustafa Y.F., Mohammed E.T., Khalil R.R., *Egypt. J. Chem.* 2021, **64**:4461 [Crossref], [Google Scholar], [Publisher]
[22]. Mustafa Y.F., *Appl. Nanosci.,* 2021 [Crossref], [Google Scholar], [Publisher]
[23]. Mustafa Y.F., Abdulaziza N.T., Jasim M.H., *Egypt. J. Chem.,* 2021, **64**:1807 [Crossref], [Google Scholar], [Publisher]
[24]. Mustafa Y.F., Abdulaziz N.T., *NeuroQuantology,* 2021, **19**:175 [Crossref], [Google Scholar], [Publisher]
[25]. Bashir M.K., Mustafa Y.F., Oglah M.K., *Syst. Rev. Pharm.,* 2020, **11**:175 [Google Scholar], [Publisher]
[26]. Mustafa Y.F., Mohammed N.A., *Biochem. Cell. Arch.,* 2021, **21**:1991 [Google Scholar], [Publisher]
[27]. Atia Y.A., Bokov D.O., Zinnatullovich K.R., Kadhim M.M., Suksatan W., Abdelbasset W.K., et al., *Mater. Chem. Phys.,* 2022, **278**:125664 [Crossref], [Google Scholar], [Publisher]
[28]. Mustafa Y.F., Bashir M.K., Oglah M.K., Khalil R.R., Mohammed E.T., *NeuroQuantology,* 2021, **19**:129 [Crossref], [Google Scholar], [Publisher]
[29]. Ismael R.N., Mustafa Y.F., Al-qazaz H.K., *Iraqi J. Pharm.,* 2021, **18**:162 [Crossref], [Google Scholar], [Publisher]
[30]. Mustafa Y.F., *Saudi Pharm. J.,* 2018, **26**:870 [Crossref], [Google Scholar], [Publisher]
[31]. Roomi A.B., Widjaja G., Savitri D., Jalil A.T., Mustafa Y.F., Thangavelu L., et al., *J. Nanostruct.,* 2021, **11**, 514 [Crossref], [Google Scholar], [Publisher]
[32]. Budi H.S., Jameel M.F., Widjaja G., Alasady M.S., Mahmudiono T., Mustafa Y.F., et al., *Braz. J. Biol.,* 2022, **84**:e257070 [Crossref], [Google Scholar], [Publisher]
[33]. Ismael R.N., Mustafa Y.F., Al-qazaz H.K., *J. Med. Chem. Sci.,* 2022, **5**:607 [Crossref], [Google Scholar], [Publisher]
[34]. Mustafa Y.F., *J. Med. Chem. Sci.,* 2021, **4**:612 [Crossref], [Google Scholar], [Publisher]
[35]. Jasim S.F., Mustafa Y.F., *Iraqi J. Pharm.,* 2021, **18**:104 [Crossref], [Google Scholar], [Publisher]
[36]. Waheed S.A., Mustafa Y.F., *Iraqi J. Pharm.,* 2021, **18**:126 [Crossref], [Google Scholar], [Publisher]
[37]. Ansari M.J., Jasim S.A., Taban T.Z., Bokov D.O., Shalaby M.N., Al-Gazally M.E., et al., *J. Clust. Sci.,* 2022 [Crossref], [Google Scholar], [Publisher]
[38]. Tasior M., Kim D., Singha S., Krzeszewski M., Ahn K.H., Gryko D.T., *J. Mater. Chem. C,* 2015, **3**:1421 [Crossref], [Google Scholar], [Publisher]
[39]. Waheed S.A., Mustafa Y.F., *J. Med. Chem. Sci.,* 2022, **5**:703 [Crossref], [Google Scholar], [Publisher]
[40]. Lv H., Tu P., Jiang Y., *Mini-Reviews Med. Chem.,* 2014, **14**:603 [Crossref], [Google Scholar], [Publisher]
[41]. Mustafa Y.F., Kasim S.M., Al-Dabbagh B.M., Al-Shakarchi W., *Appl. Nanosci.,* 2021 [Crossref],

[Google Scholar], [Publisher]
[42]. Jasim S.F., Mustafa Y.F., *J. Med. Chem. Sci.,* 2022, **5**:676 [Crossref], [Publisher]
[43]. Mustafa Y.F., Bashir M.K., Oglah M.K., *Syst. Rev. Pharm.,* 2020, **11**:598 [Google Scholar], [Publisher]
[44]. Hussien F.A.H., Keshe M., Alzobar K., Merza J., Karam A., *Int. Lett. Chem. Phys. Astron.,* 2016, **69**:66 [Crossref], [Google Scholar], [Publisher]
[45]. Bashir M.K., Mustafa Y.F., Oglah M.K., *Period. Tche Quim.,* 2020, **17**:871 [Google Scholar], [Publisher]
[46]. Kasim S.M., Abdulaziz N.T., Mustafa Y.F., *J. Med. Chem. Sci.,* 2022, **5**:546 [Crossref], [Google Scholar], [Publisher]
[47]. Mustafa Y.F., Mohammed E.T., Khalil R.R., *Syst. Rev. Pharm.,* 2020, **11**:570 [Google Scholar], [Publisher]
[48]. Mustafa Y.F., Oglah M.K., Bashir M.K., *Syst. Rev. Pharm.,* 2020, **11**:482 [Google Scholar], [Publisher]
[49]. Aldewachi H., Mustafa Y.F., Najm R., Ammar F., *Syst. Rev. Pharm.,* 2020, **11**:289 [Google Scholar], [Publisher]
[50]. Mustafa Y.F., Khalil R.R., Mohammed E.T., *Egypt. J. Chem.,* 2021, **64**:3711 [Crossref], [Google Scholar], [Publisher]
[51]. Nejres A.M., Ali H.K., Behnam S.P., Mustafa Y.F., *Syst. Rev. Pharm.,* 2020, **11**:726 [Google Scholar], [Publisher]
[52]. Cheng F., Li W., Liu G., Tang Y., *Curr. Top. Med. Chem.,* 2013, **13**:1273 [Crossref], [Google Scholar], [Publisher]
[53]. Waheed N.A., Waheed S.A., *Int. J. Pharm. Res.,* 2020 [Crossref], [Google Scholar], [Publisher]
[54]. Mustafa Y.F., Oglah M.K., Bashir M.K., Mohammed E.T., Khalil R.R., *Clin. Schizophr. Relat. Psychoses,* 2021 [Google Scholar], [Publisher]
[55]. Artursson P., Palm K., Luthman K., *Adv. Drug Deliv. Rev.,* 2012, **64**:280 [Crossref], [Google Scholar], [Publisher]
[56]. Nejres A.M., Mustafa Y.F., Aldewachi H.S., *Int. J. Pavement Eng.,* 2022, **23**:39 [Crossref], [Google Scholar], [Publisher]
[57]. Hinman S.S., Wang Y., Allbritton N.L., *Anal. Chem.,* 2019, **91**:15240 [Crossref], [Google Scholar], [Publisher]
[58]. Andrew F., Peter P., *Aust Prescr.,* 2014, **37**:137 [Crossref], [Google Scholar], [Publisher]
[59]. Zhou S.F., *Curr. Drug Metab.,* 2008, **9**:310 [Crossref], [Google Scholar], [Publisher]
[60]. Van Booven D., Marsh S., McLeod H., Carrillo M.W., Sangkuhl K., Klein T.E., et al., *Pharmacogenet. Genomics,* 2010, **20**:277 [Crossref], [Google Scholar], [Publisher]
[61]. Ghafourian T., Amin Z., *BioImpacts,* 2013, **3**:21 [Google Scholar], [Publisher]
[62]. Van De Waterbeemd H., Gifford E., *Nat. Rev. Drug Discov.,* 2003, **2**:192 [Crossref], [Google Scholar], [Publisher]
[63]. Muehlbacher M., Spitzer G.M., Liedl K.R., Kornhuber J., *J. Comput. Aided. Mol. Des.,* 2011, **25**:1095 [Crossref], [Google Scholar], [Publisher]
[64]. Mustafa Y.F., *NeuroQuantology,* 2021, **19**:99 [Crossref], [Google Scholar], [Publisher]
[65]. Benet L.Z., Hosey C.M., Ursu O., Oprea T.I., *Adv. Drug Deliv. Rev.,* 2016, **101**:89 [Crossref], [Google Scholar], [Publisher]
[66]. Raya I., Chen T., Pranoto S.H., Surendar A., Utyuzh A.S., Al-janabi S., et al., *Mater. Res.* 2021, **24**:e20210245 [Crossref], [Google Scholar], [Publisher]
[67]. Wang H., Du Y.J., Song H.C., *Food Chem.,* 2010, **123**:6 [Crossref], [Google Scholar], [Publisher]
[68]. Oglah M.K., Mustafa Y.F., *J. Glob. Pharma Technol.,* 2020, **12**:854 [Google Scholar], [Publisher]

HOW TO CITE THIS ARTICLE
Sara Firas Jasim, Yasser Fakri Mustafa. Synthesis and Antidiabetic Assessment of New Coumarin-Disubstituted Benzene Conjugates: An In Silico–In Virto Study, *J. Med. Chem. Sci.*, 2022, 5(6) 887-899
https://doi.org/10.26655/JMCHEMSCI.2022.6.3
URL: http://www.jmchemsci.com/article_148584.html